



# PTA-metrics for time-lapse analysis of well performance

A. Shchipanov<sup>1,2</sup> · L. Kollbotn<sup>1</sup> · G. Namazova<sup>3</sup>

Received: 6 December 2022 / Accepted: 3 April 2023 / Published online: 18 April 2023  
© The Author(s) 2023

## Abstract

Monitoring of a well and the surrounding reservoir performances is a crucial component in evaluating on-going and planning future well and field operations. This is carried out at all stages of a well life-span: from exploration to production and, sometimes, after abandonment. Despite tremendous progress in reservoir simulations, simple and fast techniques for well-reservoir performance evaluation are still demanded in the industry, especially in the context of the vast amount of permanent well monitoring data continuously accumulated. Such techniques are of special interest for on-the-fly well monitoring to detect and alarm about deteriorating performance issues. Installation of permanent pressure gauges in many wells motivated development of time-lapse Pressure Transient Analysis (PTA), capable of revealing and monitoring of different factors governing well performance and reservoir production. The paper describes PTA-based metrics introduced in the context of automated interpretation of time-lapse pressure responses and their derivatives. The paper begins with a review of time-lapse PTA applications in the oil and gas industry and examples of patterns formed by the time-lapse pressure transients and their derivatives in the log–log scale. Then, integral-based PTA-metrics for well-reservoir performance analysis are introduced. The metrics enable to distinguish between reservoir and well-reservoir connection contributions to a well's performance using the Bourdet derivative, while avoiding the need for selecting and matching of a well-reservoir model. The metrics were further tested with synthetic well models and field cases. The testing demonstrated high accuracy of the metrics for the cases of vertical wells with stable transient patterns. Testing for the horizontal well cases has confirmed reliability of the metrics for the stable patterns, while change of the patterns may reduce the metrics reliability. Model independence and using only pressure and rate measurements as input data are the main advantages of the metrics for integration into automated interpretation workflows and on-the-fly analysis intensively developed in the industry.

**Keywords** Well performance · Pressure transient analysis · Well testing · Time-lapse surveys · Permanent reservoir monitoring · Bourdet derivative

## Abbreviations

BU	Pressure build-up
CPI	Connection (well-reservoir) performance indicator
PTA	Pressure transient analysis
RPI	Reservoir performance indicator
WBS	Wellbore storage
WPI	Well performance indicator

## List of Symbols

$B$	Formation volume factor, dimless
$c_t$	Total (pore volume and fluid) compressibility, $\text{bar}^{-1}$
$h$	Reservoir pay thickness, m
$I_1$	Well performance indicator (WPI), $\text{bar}^{-1}$
$I_2$	Reservoir performance indicator (RPI), $\text{bar}^{-1}$
$I_3$	Well-reservoir connection performance indicator (CPI), dimless
$I_3'$	Modified well-reservoir connection performance indicator (CPI'), $\text{bar}^{-1}$
$I_1^m$	Well productivity in the model-based approach
$I_2^m$	Reservoir flow capacity in the model-based approach
$I_3^m$	Pressure drop change due to skin in the model-based approach
$k$	Permeability, mD
$L_w$	Effective well length, m

✉ A. Shchipanov  
ansh@norce-research.no

<sup>1</sup> NORCE, Stavanger, Norway

<sup>2</sup> University of Stavanger, Stavanger, Norway

<sup>3</sup> Wintershall Dea, Stavanger, Norway

$p$	Pressure, bar
$p_i$	Initial pressure for transient, bar
$PI$	Productivity index, $m^3/(day \cdot bar)$
$\Delta p$	Pressure drop, bar
$\Delta p'$	The Bourdet derivative of the pressure, bar/hr
$\Delta p_S$	Pressure drop due to skin, bar
$\bar{p}$	Average reservoir pressure, bar
$Q$	Rate, $m^3/day$
$r_w$	Wellbore radius, m
$S$	Well skin, dimless
$t$	Elapsed time, hr
$t_{ref}$	Current elapsed time, hr
$X_f$	Induced fracture half-length, m
$\phi$	Porosity, frac.
$\mu$	Fluid viscosity, cp

### Indices

base	Reference transient in time-lapse sequence
$D$	Dimensionless parameter

## Introduction

Installation of permanent downhole gauges (PDG) and flow meters in the petroleum and other industries and accumulating big sets of well surveillance data have provided a basis for breakthrough in well and reservoir monitoring (Horne 2007). A progress in well monitoring was recently achieved through development and application of time-lapse pressure transient analysis (PTA) and deconvolution methods. PTA is a powerful tool for well performance evaluation, separating wellbore, near-well, inter-well and reservoir boundary effects and classifying their contributions (Bourdet 2002), (Gringarten 2008), (Houze et al. 2020). Time-lapse PTA focuses on all these effects and their evolution during a well life-span, while deconvolution aims mainly at reproducing long-term pressure transient responses including distant boundary effects. Hereafter, we concentrate on time-lapse

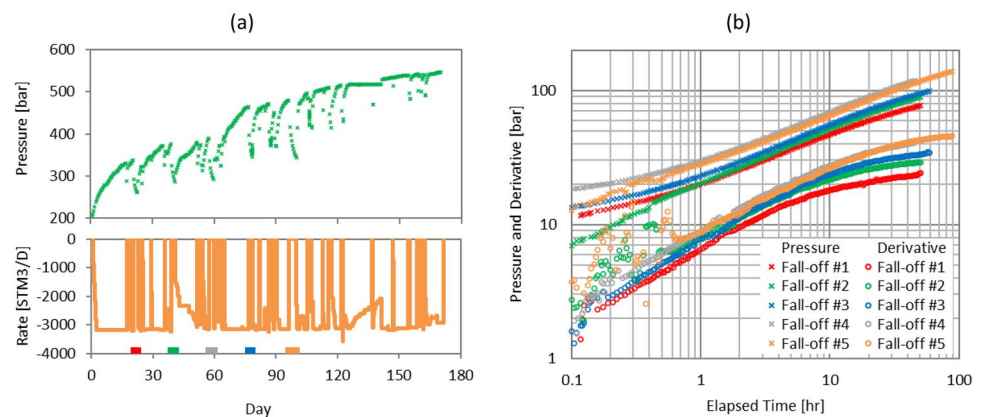
PTA with many different applications reported, mainly for the petroleum industry, while the progress and applications of deconvolution are very well covered in the literature (Gringarten 2008), (Whittle et al. 2009), (Cumming et al. 2014).

Permanent well and reservoir surveillance with PDG and time-lapse PTA is today employed in the oil and gas industry with focus on well performance and behavior with their changes during reservoir life-time, including fluid contact movements and recovery processes (Gringarten et al. 2003), (Yaich et al. 2012), (Ugoala et al. 2013), (Rushatmanto et al. 2017), (Suleen et al. 2017), (Cassie et al. 2018); well stimulations (e.g., acid and fracture jobs) and monitoring of well performance over time (Shchipanov et al. 2014), (Shchipanov et al. 2017a, 2017b); and any kind of improved/enhanced oil recovery pilots such as water shut-off (Aamodt et al. 2018) and silicate injection (Skrettingland et al. 2012), (Skrettingland et al. 2014). Figure 1 illustrates typical time-lapse pressure transient responses for sequential well shut-ins from (Shchipanov et al. 2017a).

Hereafter, we review a part of these applications for conventional oil and gas reservoirs, which may be described as the cases of dominating low-compressible single-phase flow in the reservoir such as initial oil production before water- or gas-breakthrough or water injection after forming of an injection pattern. In this context, dominating means that the area around the well in focus is mainly saturated with a single movable low-compressible fluid (like oil or water), while other movable fluids may be present at some distance from the well. This limited application area is governed by using the pressure formulation in the log–log plot (commonly used in PTA of oil and water wells) in contrast to the pseudo-pressure formulation integrating fluid PVT properties in the log–log plot used for gas wells (Bourdet 2002).

Among many oil field studies employing time-lapse PTA, the following ones may be highlighted to illustrate the wide range of applications. Interpretation of real-time pressure measurements was used as a component in the survey of sodium silicate injection pilot (Skrettingland, Giske et al.

**Fig. 1** Injection history **a** and time-lapse pressure transient responses for five well shut-ins **b** observed in the well history (Shchipanov et al. 2017a)



2012) (Skrettingland et al. 2014). Here time-lapse pressure fall-off analysis was used to monitor the silicate placement in the inter-well area by interpreting the continuous increase in flow resistance. Analysis of long horizontal wells with multiple fractures revealed the value of integrating both flowing and shut-in periods in the time-lapse PTA (Shchipanov et al. 2014). The value of combining flowing and shut-in analyses was highlighted previously the context of improved reliability in evaluations of fault conditions (sealing or leaking) in compartmentalized reservoirs (Larsen 2005). Shchipanov et al. (2014) have shown that flowing periods may be different from shut-ins due to dynamic reservoir behavior related to induced fractures, rock mechanics and wellbore cross-flows. The difference may also help in disclosing well interference effects. Further study (Shchipanov et al. 2017b) has extended the scope of time-lapse PTA to deal with multiple rate pressure transients and step-rate test analysis to monitor performance of wells with induced fractures. Aamodt et al. (2018) discussed water shut-off jobs with massive cement placement into an injection well to improve water conformance control, where permanent pressure surveillance and PTA, including combined flowing/shut-in analysis, were used to identify well communication and to monitor the job efficiency. Recent field study by Walker et al. (2021) employed time-lapse PTA to monitor initial phase of production in a giant oil field, where well interference and boundary conditions of the reservoir were disclosed from analysis of time-lapse flowing and shut-in periods. The invention of wireless pressure gauges has opened new perspectives for post-P&A well monitoring. In an application of the wireless measurements, Champion (20162016) has shown that post-P&A well pressure monitoring extends the radius of investigation of exploration wells and improves the understanding of distant flow barriers and therefore production potential. Wireless pressure measurements may also be used for time-lapse analysis, concentrating on wellbore and reservoir leakages, active nearby wells and reservoir boundaries.

All these field applications have demonstrated the high potential of time-lapse PTA for permanent well and reservoir monitoring highlighting capabilities to address a variety of problems from routine well performance monitoring to understanding of dynamics of faults and fluid contact movements as well as supporting IOR/EOR pilots and applications. The main approach in these applications is comparison of time-lapse pressure transient responses and their derivatives in log–log scale or ‘families of transients’ such as illustrated by Fig. 1. The applications mentioned above used a model-driven approach to interpret the observed data, which is based on selecting a representative reservoir simulation model (analytical or numerical) for describing well and reservoir segment in focus and to match the observed pressure transients. Such approach requires detailed description of the well (schematics, completion details) and the reservoir

(geological environment like structure, faults etc.) as well as fluid PVT data, accompanied by manual interpretation and simulations with significant manpower and resources required. In practice, such interpretations are usually carried out only for selected wells and particular data windows of interest (e.g., well stimulations and treatments, significant production/injection impairment observed, etc.). Such time-lapse analysis is also often limited to shut-in data, which are easier to interpret, leaving vast amount of well flowing data out of the scope.

Practical interpretation of PDG data has many challenges including ability to process big datasets; data denoising, synchronizing and smoothing; and identifying of pressure transients (Suzuki 2018), (Moosavi et al. 2018), (Zhang et al. 2021), (Guo, et al. 2021). The patterns formed by pressure transients and their derivatives are in focus of different studies (see for example, Mimoun and Fernandez-Ibanez 2023), but attracted special interest in the automated workflows (Suzuki 2018).

The large amount of available well monitoring data and challenges to utilize all those data with conventional manual interpretation technique has disclosed a need for specific automated approaches for PDG data interpretation. Such approaches may have a limited level of detail in description of well performance, at least at the first stage, which enables automation. In a first approximation, such a description may be independent of well completion details and fluid PVT data, providing a basis for flexible wide-range applications. Such automated analyses would not substitute the manual interpretation described above, but rather provide environment for manual interpretations highlighting well and reservoir performance issues at the full well life-span.

This paper focuses on suggesting and testing metrics based on the knowledge gained from PTA for time-lapse monitoring of well and reservoir performances. The metrics should fulfill requirements for automated interpretation of big datasets and on-the-fly analysis with early alarms on performance issues calling for fast and model-independent solutions. Using such metrics in automated interpretation workflows should help to uncover huge amount of information contained in permanent pressure measurements. Hereafter, we do not attempt to cover the whole wide range of the applications reviewed above, but consider a limited range of applications commonly met in the field studies (such as performance of vertical and horizontal wells), which is considered as a natural first step on the way ‘from simple to complex’.

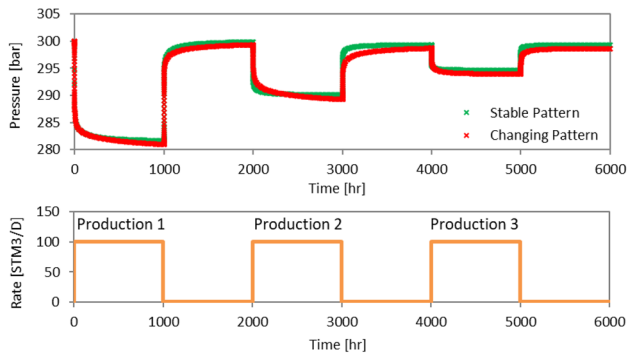


**Fig. 2** Synthetic time-lapse well survey consisting of three production and shut-in periods simulated to illustrate stable (green) and changing (red) patterns of time-lapse responses in the log–log plot in Figs. 3, 4

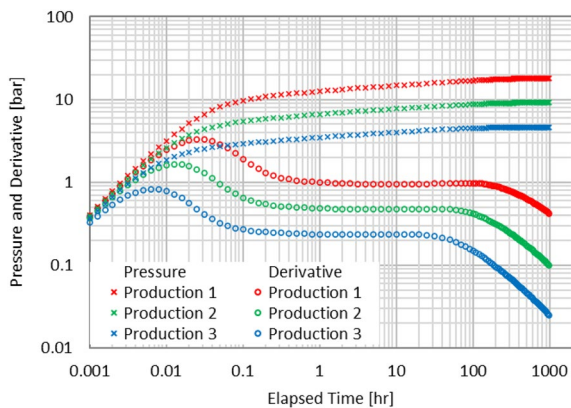


**Fig. 3** Stable pattern in the log–log plot formed by the time-lapse pressure transient responses and their derivatives from Fig. 2 (production periods, green pressure history). Flow capacity, kh, is changing from 1000 mD.m (production #1) to 2000 (production #2) and 4000 (production #3). The case of infinite reservoir with a fault with constant pressure boundary condition

## Patterns in time-lapse pressure transient responses

Time-lapse PTA focuses on analysis of the patterns formed by the pressure transients and their Bourdet derivatives as illustrated in (Figs. 2, 3, 4). Here, if the well and reservoir performance remain unchanged with time, all the transients (derivatives) should coincide. Exceptions may be found in comparison of flowing and shut-in responses, where shut-in transient and derivative may deviate from flowing ones, or even may have opposite slope for late-time derivative responses as in the case of the closed chamber reservoir (Bourdet 2002). Taking the exceptions above, in most of the cases: if well and/or reservoir performance start to change, the transients start to deviate from each other (Fig. 3), which is used in time-lapse PTA to analyze such changes in the

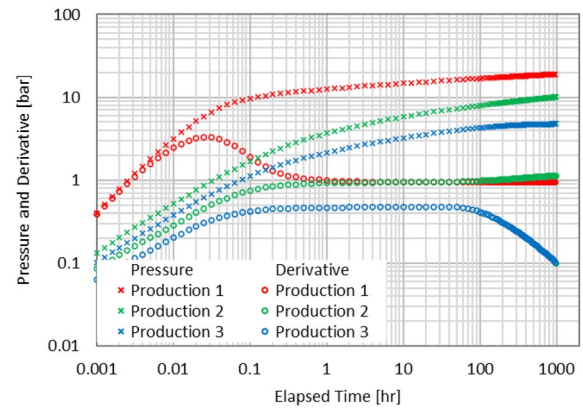


**Fig. 4** Changing pattern in the log–log plot formed by the time-lapse responses from Fig. 2 (production periods, red pressure history). The parameters for different production periods: 1000; 0; ‘infinite’ (production # 1), 1000; 30; ‘infinite’ (production # 2) and 2000; 30; ‘pressure’ (production # 2), where the first parameter is flow capacity, kh [mD.m]; second is  $X_f$ -induced fracture half-length [m] and third parameter is boundary condition: infinite reservoir (‘infinite’) or reservoir with a fault with constant pressure boundary condition (‘pressure’)

well performance. Depending on changes, two alternatives may be observed: stable or changing pattern. Stable pattern may be observed, for example, when some reservoir properties are changed (like permeability in Fig. 3). Change of well performance, such as in the case of induced fracturing (comparing blue and orange curves as shown in (Fig. 4), may lead to appearance of a changing pattern. The pattern in Fig. 4 changes further due to permeability increase and connection to an aquifer (the green curves) simulated using the constant pressure boundary condition on one of the reservoir boundaries.

As far as time-lapse pressure transient responses and their derivatives form patterns in the log–log plot, metrics may be suggested to get quantitative measures characterizing changes of well and reservoir performance based on analysis of the patterns. One could also guess that stability and variability of the patterns are important characteristics influencing the application of such metrics.

## PTA-metrics for well and reservoir performance suitable for time-lapse analysis

Productivity (or injectivity) index,  $PI$ , is a simple concept widely used in reservoir engineering practice to analyze and compare well performances (Bourdet 2002), (Houze et al. 2020). This index is usually calculated as the ratio of the well production rate to difference between the average reservoir pressure in the well drainage area and the well flowing pressure (Bourdet 2002):

$$PI = \frac{Q}{\bar{p} - p(t)} \quad (1)$$

The average pressure is equal to the initial reservoir pressure for start of production from a virgin reservoir. It may also be approximated by the initial pressure for a transient, but the accuracy of such  $PI$  calculation depends on the deviation of the initial transient pressure from the average pressure. Using the productivity index does not allow for separating well and reservoir effects, which is valuable information for well performance analysis and, especially, for forecasting the well performance and planning operations such as well stimulations, treatments and adjusting rates for other wells. Suggesting indicators like  $PI$  for well performance analysis which enables distinguishing between well and reservoir effects is therefore of practical interest.

The pressure derivative suggested by D. Bourdet with co-authors (Bourdet et al. 1989) has opened a new dimension in well and reservoir performance analysis allowing for separating well and reservoir effects. This also enabled more efficient characterization of different flow regimes (comparing to classical type-curve analysis) governed by different well and reservoir features such as fractures, faults, fluid contacts and many others (Bourdet 2002).

Analysis of well performance may be considered on the example of production from a vertical well in an infinite reservoir. In this case, the approximate analytical solution for pressure drawdown after the start of single-phase production at constant rate,  $Q$ , may be obtained in the following form based on the one-dimensional solution in the radial coordinates (Bourdet 2002):

$$\Delta p = p_i - p(t) = 21.49 \frac{QB\mu}{kh} \left( \log(t) + \log \frac{k}{\phi\mu c_i r_w^2} - 3.098 + 0.87S \right) \quad (2)$$

Differentiating the solution (2) gives the relationship linking the reservoir flow capacity or permeability-thickness product,  $kh$ , with the fluid properties ( $B$  and  $\mu$ ) and the Bourdet derivative of the pressure drop:

$$kh = 21.49QB\mu \left( \frac{d(\Delta p)}{d(\log(t))} \right)^{-1} \quad (3)$$

The transient  $PI$  formulation may also be obtained based on (1) and the solution (2) above, assuming  $\bar{p} \approx p_i$  in the form:

$$PI = \frac{Q}{\Delta p} = kh \left( 21.49B\mu \left( \log(t) + \log \frac{k}{\phi\mu c_i r_w^2} - 3.098 + 0.87S \right) \right)^{-1} \quad (4)$$

For stabilized pressure drop, e.g., in the case of constant pressure external boundary, the productivity index becomes

proportional to the ratio of the flow capacity to the fluid properties:  $PI \sim kh/B\mu$ .

Integral characteristics are traditionally used in production (or rate transient) analysis (Blasingame et al. 1991), (Houze et al. 2020) and were also previously suggested to analyze noisy well test data (Blasingame et al. 1989). The idea of integrating well response data over time may also be adapted to time-lapse PTA to reduce effect from noise in pressure measurements, while keeping signature of long-term reservoir response. This has motivated the search of possible criteria based on the integral characteristics, suitable for large and noisy pressure data sets, which may be used as metrics in comparison of time-lapse well responses.

Since permanent pressure and rate measurements (usually with different sampling rates) are widely available from the PDG/flow meters installed in new wells, we can focus exclusively on these data sets. In this case, time-lapse analysis of the well performance may be carried out via plotting pressure transient response to a production (injection) with a given rate. The following integral-based performance indicators may be calculated based on the areas under pressure drop,  $\Delta p$ , the Bourdet pressure derivative  $\Delta p'$  and a back calculated parameter as:

$$I_1 = \left( \frac{Q_{base}}{Q} \frac{1}{t_{ref}} \int_0^{t_{ref}} \Delta p dt \right)^{-1} \quad (5)$$

$$I_2 = \left( \frac{Q_{base}}{Q} \frac{1}{t_{ref}} \int_0^{t_{ref}} \Delta p' dt \right)^{-1} = \left( \frac{Q_{base}}{Q} \frac{1}{t_{ref}} \int_0^{t_{ref}} \frac{d(\Delta p)}{d(\log(t))} dt \right)^{-1} \quad (6)$$

$$I_3 = I_1/I_2 \quad (7)$$

The relationship (6) is valid for the first production period as discussed above, while the logarithmic time,  $\log(t)$ , should be replaced by the superposition time for multiple rate of well shut-in cases (Bourdet 2002). These indicators include the scaling to the reference rate in a family of time-lapse transients,  $Q_{base}$ , a standard procedure for comparison of time-lapse responses.

The first integral above,  $I_1$ , may be used as the well performance indicator (WPI), similar to the  $PI$  formulation (4), assuming that the pressure drop in the transient is close to the drop between bottom hole pressure and average reservoir pressure in the drainage area. The second integral,  $I_2$ , may serve the reservoir performance indicator (RPI). Following (3), the Bourdet derivative is inverse proportional to the reservoir flow capacity. Therefore, the integral of the Bourdet derivative (6) reflects the reservoir flow capacity for the case of production from a vertical well. The areas below the pressure drop and derivative curves in (5) and (6), calculated via integrating with respect to the elapsed time, reflect well and

reservoir performances: the smaller the area, the higher the performance.

The third parameter,  $I_3$ , may be considered as the well-reservoir connection performance indicator (CPI). This parameter originates from the difference between the pressure drop curve and its Bourdet derivative in the log–log scale, which includes skin-related pressure drop (negative of positive) on top of a difference observed for a well without skin:

$$I_3' = \left( \frac{Q_{base}}{Q} \frac{1}{t_{ref}} \int_0^{t_{ref}} [\log(\Delta p) - \log(\Delta p')] dt \right)^{-1} \quad (8)$$

The formulation (8) is a proxy of the formulation (7) in the form  $I_3' \sim [-\log(I_3)]^{-1}$ , but (7) doesn't require calculation of the integral in (8) and satisfies the relationship:

$$I_1 = I_2 \cdot I_3 \quad (9)$$

The relationship (9) makes the logic of the metrics (5–7) clear: the overall well performance is the product of reservoir and well-reservoir connection performances. The formulation (7) has also an advantage compared to (8) in reducing the computational time. The ratios of CPIs calculated by (7) and (8) in time-lapse analysis are often close to each other as illustrated in the example below. Both CPI formulations (7) and (8) may be used in time-lapse PTA, although (7) is prioritized in this paper taking the advantage of the metrics logic by fulfilling (9).

Well performance monitoring may be carried out in practice through applying dimensionless WPI, RPI and CPI indicators, normalized to a chosen reference transient (denoted with 'base' index below):

$$I_{i,D} = I_i / I_{i,base}, i = 1, \dots, 3 \quad (10)$$

Verification of the metrics via comparison with the results of the conventional model-based PTA interpretation requires introduction of equivalent performance indicators based on the model parameters. The following indicators were used to compare the PTA-metrics with the results of the model-based approach:

$$I_1^m = \frac{Q}{\Delta p}, \quad (11)$$

$$I_2^m = kh, \quad (12)$$

$$I_3^m = \frac{\Delta p - \Delta p_s}{\Delta p}, \quad (13)$$

$$I_{i,D}^m = I_i^m / I_{i,base}^m, i = 1, \dots, 3 \quad (14)$$

**Table 1** Table of comparison of the PTA-metrics (10) with the model-based metrics (14) for well, reservoir and connection performances as used further in the paper. Comparison of the 'model-based' and 'PTA-metrics' columns may be used to evaluate accuracy of the PTA-metrics as deviation from the model-based metrics

Well performance		Reservoir performance		Connection performance	
Model-based	PTA-metrics	Model-based	PTA-metrics	Model-based	PTA-metrics
$I_{1,D}^m$	$I_{1,D}$	$I_{2,D}^m$	$I_{2,D}$	$I_{3,D}^m$	$I_{3,D}$

where  $I_1^m$ ,  $I_2^m$  and  $I_3^m$  define the well productivity, the reservoir flow capacity and the change of pressure drop due to skin, where the index 'm' means 'model-based'. (14) is the equivalent dimensionless form of the indicators to those in (10). The dimensionless indicators (14) resulted from the model-based approach may be compared to the PTA-metrics indicators (10). The synthetic examples followed by the field cases in the next sections focus on comparison of the metrics (10) and (14) as illustrated in Table 1 for the cases of production (injection) from vertical wells including skin and wellbore storage effects as well as production from horizontal wells.

## Testing PTA-metrics with synthetic well examples

The PTA-metrics for well-reservoir performance analysis were first tested on synthetic well examples. The objective was to study how the suggested performance indicators reflect known changes in reservoir (governed by change of reservoir flow capacity,  $kh$ ) and well connectivity (driven by well skin) performances. In all the cases below, well flowing pressure transient response to a constant rate (the same in all the cases) was simulated in the Saphir software and further analyzed comparing the metrics (10) and (14).

The first three examples of the PTA-metrics testing are the cases of two vertical wells (the first well is the reference one, the second—the same well, but with one modified parameter like  $kh$  or skin) in an infinite homogeneous reservoir without wellbore storage (WBS) effect as illustrated in Fig. 5 through Fig. 7. In the first case, change of the flow capacity,  $kh$ , is analyzed (Fig. 5). Here, the doubling of  $kh$  for the second well is reflected by the doubling of the Reservoir Performance Indicator (RPI), while absence of skin changes is also reflected by the Connection Performance Indicator (CPI), which remains close to unity (0.96). Transient WPI and CPI gradually approach the 'true solution' at late time of the transient as it is shown in Fig. 5c. Two alternative

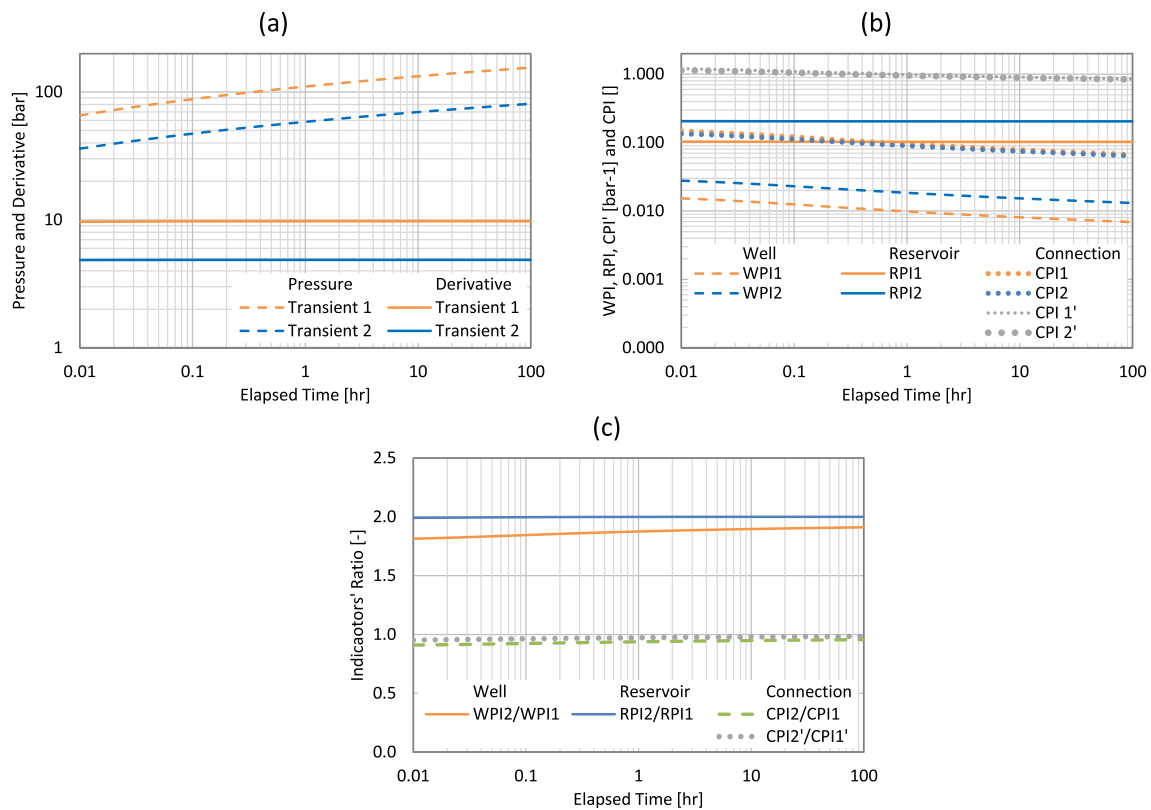


**Fig. 5** Well performance analysis of two vertical wells (without WBS) with twice different  $kh$  and the same zero skin. Three plots depict the following for the compared wells: **a** Pressure and derivative transients; **b** Well, reservoir and connection performance indica-

tors (WPI, RPI, CPI and CPI'); **c** Ratio of the performance indicators (dimensionless indicators). Dimensionless WPI, RPI and CPI (CPI') after 100 h: 1.91, 2.00, 0.96 (0.98)

**Table 2** Comparison of the PTA-metrics (10) with the model-based metrics (14) for well, reservoir and connection performances for the results shown in Figs. 5, 6, 7, 8

Transients compared	Well performance		Reservoir performance		Connection performance	
	Model-based	PTA-metrics	Model-based	PTA-metrics	Model-based	PTA-metrics
Figure 5	2.00	1.91	2.00	2.00	1.00	0.96
Figure 6	0.50	0.49	1.00	1.00	0.50	0.49
Figure 7	2.00	2.16	1.00	1.01	2.00	2.14
Figure 8	1.00	0.97	2.00	1.92	0.50	0.50

formulations for CPI calculations, using (7) for CPI and (8) for CPI', were compared in this example: both CPIs behave similarly providing very close CPI ratios (Fig. 5b), although CPI' is 2% more accurate than CPI (Fig. 5c). Taking the advantages of the metrics (5)-(7) compared to (5), (6), (8) described above, the first metrics are further applied in this paper, although application of the PTA-metrics may also include (8) as an alternative CPI. Table 2 illustrates comparison of the results of the metrics (10) and (14) for the synthetic cases.

The second and third cases focused on modifying of the well skin in both directions. The skin variation from 0 to 8 and from 0 to -4.2 caused doubling of the pressure drop in the second case and twice lower pressure drop in

the third case for the second wells. The change of pressure drop due to skin is properly reflected by CPIs as shown in Fig. 6 (positive skin) and Fig. 7 (negative skin). Here, RPI remains close to unity showing almost no change in reservoir performance reflecting no change of flow capacity in the simulations ('true solution'). It should be noted that although the final indicators (at the end of a transient) and their ratios are quite close to the 'true solution' governed by specified changes of  $kh$  and skin, the ratios may deviate significantly from the 'true solution' for the early time periods (Figs. 6, 7). Here, establishing a flow regime reflected in stabilization of the derivative trend (radial flow regime in this case) is crucial for proper evaluation of the indicators, as illustrated by Fig. 7 with large derivative deviation at early time due to

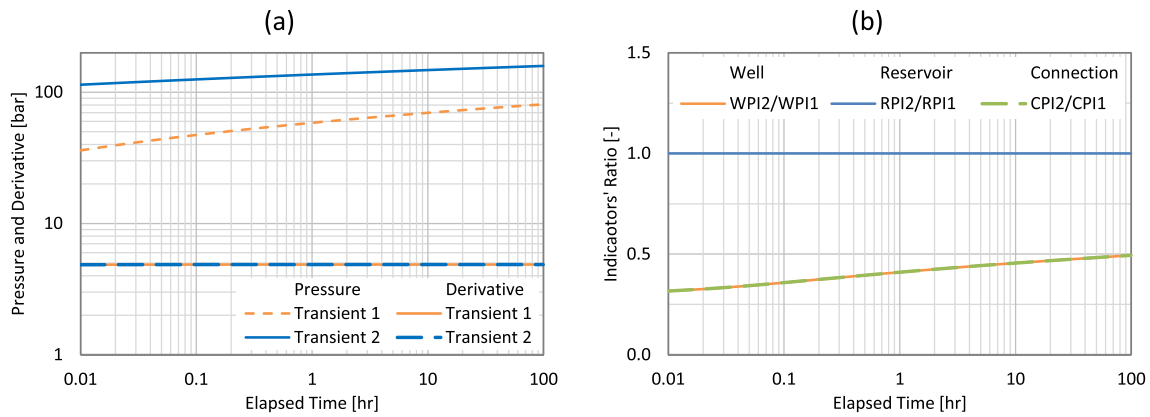


**Fig. 6** Similar well performance analysis (Fig. 5) for two vertical wells, but with the same  $kh$  and different skins: 0 and 8, the last skin provides twice higher pressure drop at end of the transient. Pressure

and derivative transients **a** are followed by ratio of the performance indicators **b**. Dimensionless WPI, RPI and CPI at the end of the transients are 0.49, 1.00 and 0.49

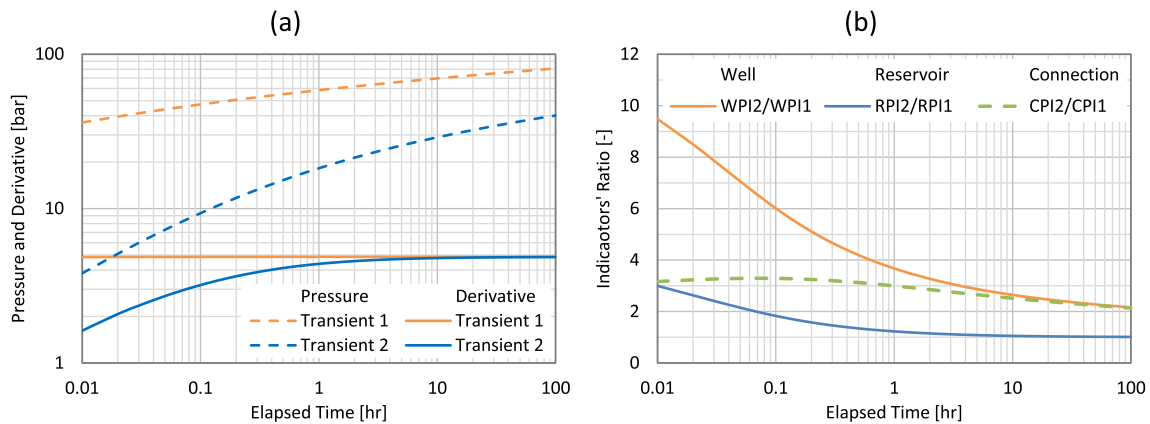


**Fig. 7** Similar well performance analysis (Fig. 6), but for zero and negative skins: 0 and  $-4.2$  (e.g., induced fracture impact), the last skin provides twice lower pressure drop at end of the transient. Dimensionless WPI, RPI and CPI at the end of the transients are 2.16, 1.01 and 2.14

large negative well skin. At the same time, if the early time flow regime has limited duration, the integral manner of the indicator' calculations would minimize the deviation from the 'true solution'. Overall, the PTA-metrics provided reliable indicators in all the cases of the vertical wells without WBS in Figs. 5, 7.

As a next step, vertical wells with WBS effect were considered in the synthetic case illustrated in Fig. 8. This case is a combination of the cases shown in Figs. 5, 6 with the WBS effect. Here, the second well has doubled  $kh$ , which should provide twice lower pressure drop. At the same time, simultaneous increase in the skin from 0 to 8 (providing additional pressure drop to the overall drop for the doubled  $kh$  case) brings the overall pressure drops for the second and first wells to the same level. The PTA-metrics properly reflect all the  $kh$  and skin-related pressure drop changes (Fig. 8). The presence of the wellbore storage causes some deviations of the well and reservoir performance indicators from 'true

solution', but this deviation is moderate and declines during the main (radial) flow regime (does not exceed 5% at 100 h).

Evaluation of the PTA-metrics accuracy for all the synthetic cases above (Figs. 5, 6, 7, 8) may be carried out based on the results summarized in Table 2. The PTA-metrics provide quite accurate estimates for all the indicators in all the cases: average (maximum) error of 4 (8) % for WPI and 1 (4) % for RPI and 3 (7) % for CPI. The accuracy is a function of early-time disturbance of the transients caused by negative skin and WBS effect. It should be also mentioned that WPI according to (5) accounts for curvature of the pressure drop curve, which is not accounted in (11). The accounting for the pressure drop history may be rather considered as advantage of the formulation (5) in comparison with (11), also influencing the error evaluation above.

The metrics (10) and (14) have theoretical background in the solutions obtained for production from a vertical well in an infinite reservoir. Keeping this assumption in mind,



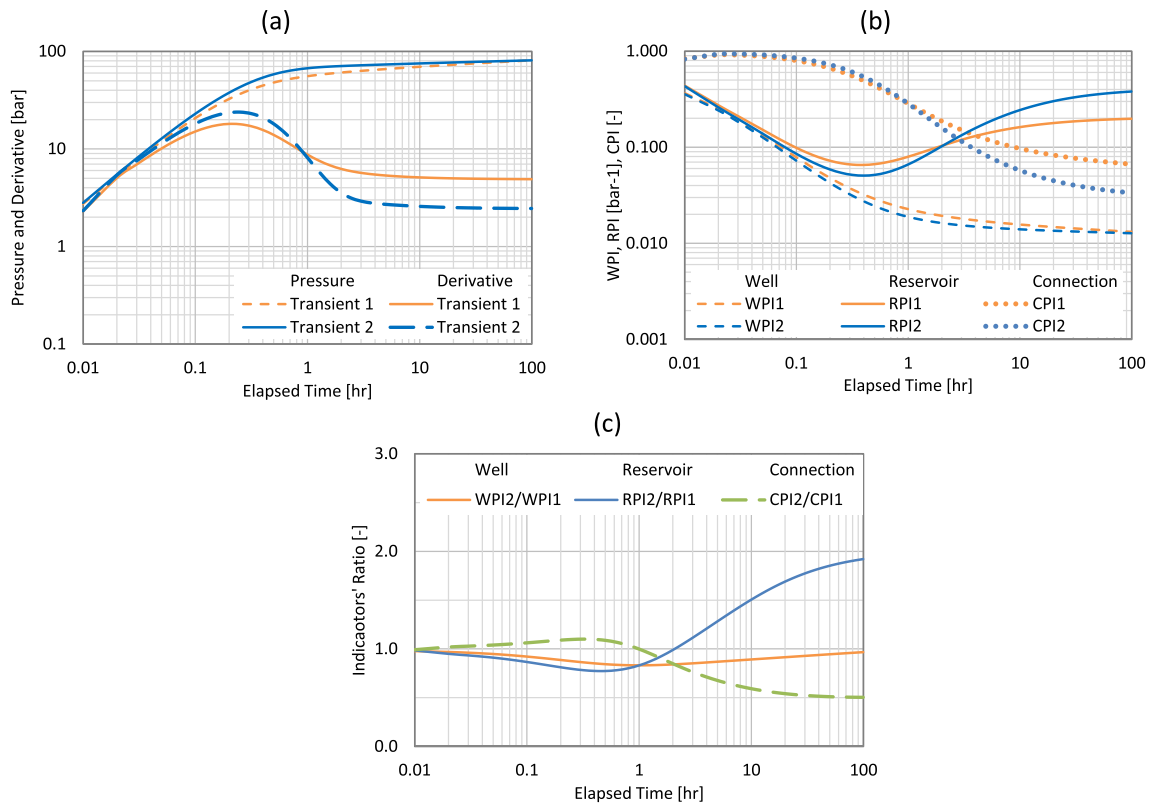


**Fig. 8** Performance analysis for two vertical wells with WBS effect: the second well has doubled  $kh$  and increased skin (8, changed from 0 for the first well). This combination of parameters, however, provides

the same pressure drop at end of the transients. Dimensionless WPI, RPI and CPI at the end of transient period are 0.97, 1.92 and 0.50

these metrics may also be tested for the case of production from a horizontal well. This case is of interest due to wide application of horizontal well drilling in the industry today. Such application of the PTA-metrics to more complex case of a synthetic horizontal well was also considered as an introduction to the second field case discussed below. As an illustration of non-uniqueness of the response interpretation

in the case of horizontal well, the reference well response (Transient 1) was compared to three cases of modified well and reservoir parameters: the case with doubling of permeability,  $k$  (Transient 2), reservoir pay thickness,  $h$  (Transient 3) or doubling of the effective (flowing) well length (Transient 4) as shown in Fig. 9 (skin is zero in all the cases). The time-windows in Fig. 9 (and following figures in the paper)

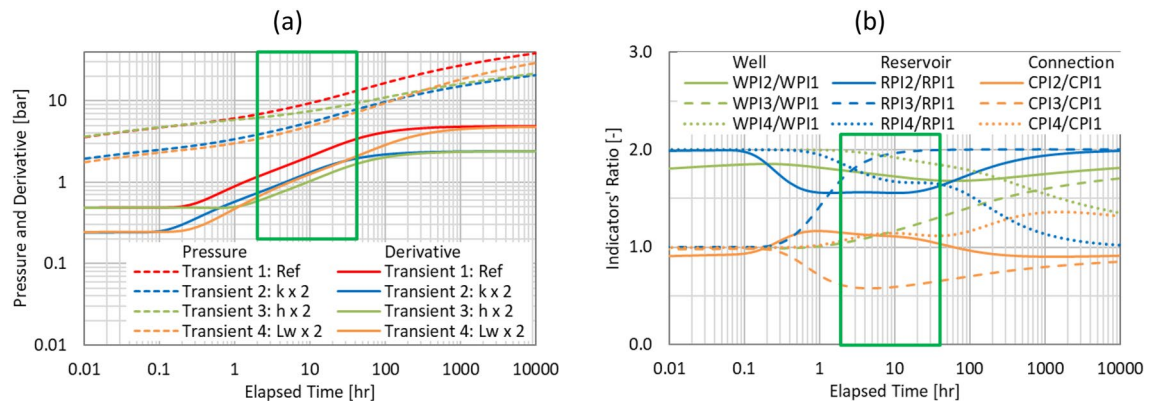


**Fig. 9** Similar well performance analysis (Fig. 8, a and c) for a horizontal well without WBS and zero skin (Transient 1, reference) and the same well response but with doubled permeability,  $k$  (Transient 2), reservoir pay thickness,  $h$  (Transient 3) and effective well length,  $L_w$  (Transient 4)

highlight periods with stable pressure derivative patterns. Representative performance indicators are calculated at the end of such periods.

In reality, the late-time response (as observed after 40 h in the log–log plot in Fig. 9a) is difficult to observe due to geometry of horizontal wells, interference with nearby wells and reservoir boundaries as it will be shown in the field case discussed below. In this context, we could first compare the transients within duration of 40 h in Fig. 9 as the most representative case of the horizontal well responses. The comparison revealed minor difference between the pressure derivatives of the responses of the modified cases within the stable pattern time-window. In certain context,  $kh$  was doubled in all the modified cases: as  $kh$  in the cases of the transient 2 and 3 and as  $kh$  of equivalent vertical well producing between two sealing faults for the transient 4. Therefore, the derivatives of these cases look similar. In the long-term perspective, the picture changes: the cases of doubling  $k$  or  $h$  will tend to a response of vertical well in a reservoir with doubled  $kh$ , while doubling of the well length converges to the case of a vertical well in the same  $kh$  reservoir. These cases showed that application of the metrics has common for PTA limitation: knowledge gained from a transient is always limited by its duration and flow regimes observed. At the same time, the metrics give reliable evaluation taking this limitation into account. From interpretation point of view, observing the derivative before 40 h may be interpreted as

increasing  $kh$  or effective well length, while the late response (100–1000 h) gives clear indication of what was actually changed in these cases.

The horizontal well analysis has shown that if multiple flow regimes occur (like early radial, linear and late radial flow regimes for the horizontal wells in focus) interpretation of well and reservoir performance becomes time-dependent (governed by duration of a transient) as well as complicated in terms of defining a unique solution. Nevertheless, the PTA-metrics still provide reliable qualitative evaluation, showing proper trend of the indicator' changes and their approximate quantitative measures (Table 3). The deviations from the model-based performance (which can't be considered as 'true solution' in contrast to the vertical well cases) may be explained by multiple flow regimes occurred (a complex well response). It should be noted that WPI is quite close to  $PI$  in all the cases, while RPI is very close to  $kh$  for transient 3 and CPIs properly demonstrate no skin changes for the transients 2 and 4.

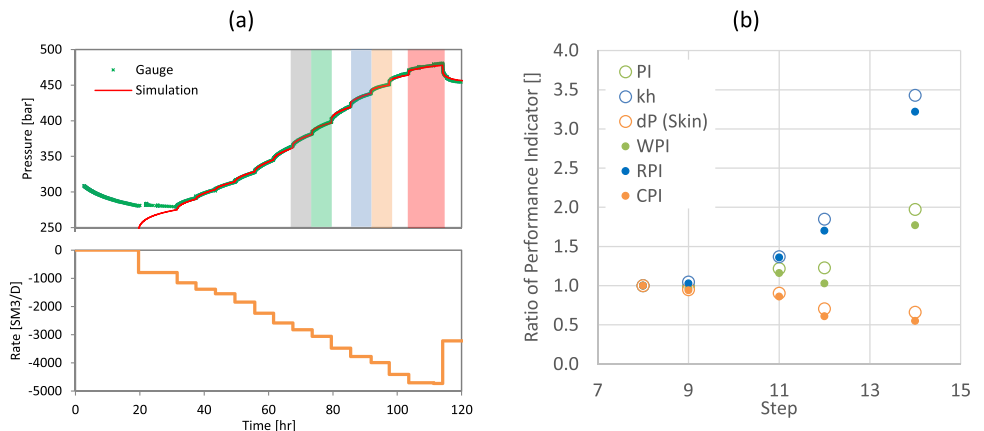
### Testing on multi-rate field data

A multi-rate or step-rate test of a slanted fractured injection well from the study (Shchipanov et al. 2017b) was chosen as the first real data set for testing of the PTA-metrics. The multi-rate test is a time-lapse PTA survey with sequential

**Table 3** Comparison of the PTA-metrics (10) with the model-based metrics (14) for well, reservoir and connection performances for the results shown in Fig. 9. The indicators reflect changes in the performance in comparison with Transient 1 (the reference horizontal well)

Transients Compared	Well performance		Reservoir performance		Connection performance	
	Model-based	PTA-metrics	Model-based	PTA-metrics	Model-based	PTA-metrics
Transients 2: $k \times 2$	1.67	1.69	$k \times 2$	1.63	1.00	1.04
Transients 3: $h \times 2$	1.39	1.31	$h \times 2$	1.99	1.00	0.66
Transients 4: $L_w \times 2$	1.81	1.85	$L_w \times 2$	1.65	1.00	1.12

**Fig. 10** Step-rate test of a slanted fractured well **a** and comparison of manual step-by-step PTA interpretation (dimensionless  $PI$ ,  $kh$  and  $dP$  (Skin) according to the metrics (14)) and results of the PTA-metrics application (dimensionless WPI, RPI and CPI, according to (10)) as deviations from the reference values at step 8 **b**. **a** Also shows simulated pressure with the estimated well-reservoir parameters (Shchipanov et al. 2017b)



flowing periods. The well penetrates naturally fractured reservoir and was stimulated to create an induced fracture. A well test was taken during water injection, consisting of a sequence of 14 steps of increasing injection rate with almost constant rate stepping and duration of each step, excluding the first and last steps (Fig. 10a). The well bottom hole pressure measured by a permanent downhole gauge was not equilibrated before the well test causing some pressure disturbance at the first steps due to previous injection. The main objective of such well tests is usually to monitor induced fracture, but they may also be interpreted using the step-by-step (time-lapse) approach (Shchipanov et al. 2017b) to evaluate changes of reservoir flow capacity,  $kh$  and skin from manual PTA of transients from all the steps.

In this paper, the results of such interpretation from (Shchipanov et al. 2017b), which are the deviations of  $kh$ , skin and injectivity index ( $PI$ ) at each step from the values obtained for the reference step (step 8) (converted into the metrics (14) (Fig. 10b) were compared to results of PTA-metrics application (10) to the same well test data. The objective was to verify the ability of the PTA-metrics to reproduce the results of the manual PTA interpretation.

The steps 8, 9, 11, 12 and 14 were chosen to test the PTA-metrics since these steps demonstrated changes in the well performance, mainly due to increasing flow capacity,  $kh$  (Fig. 11a). Application of the PTA-metrics (Fig. 11b) gave results, which are quite close to the manual interpretation results (Fig. 10b) with maximum (average) deviations of 16 (8) % for WPI, 8 (4) % for RPI and 17 (9) % for CPI (Table 4). The analysis has confirmed capabilities and acceptable accuracy of the metrics for applications to vertical /slanted fractured wells, where radial flow regime is observed.

### Testing on time-lapse shut-in field data

The PTA-metrics were then tested on a real field case of a horizontal production well, where time-lapse PTA was previously applied to characterize well interference and impact of injection on reservoir performance (Molina 2020), (Namazova et al. 2021). These studies focused on the Southern part of a fault-block reservoir, penetrated by three horizontal producers and one injector, where injection started after a year of depletion period (Figs. 12, 13).

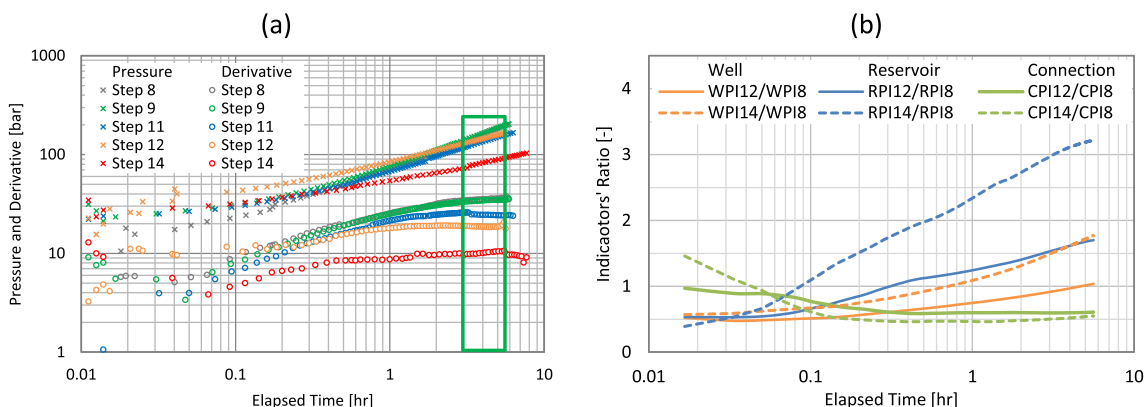


**Fig. 11** Log–log plot of the pressure transients measured at steps 8, 9, 11, 12 and 14 **a** and dimensionless well, reservoir and connection performance indicators for steps 12 and 14 as ratios to the reference values for step 8 **b**. The green square in **a** highlights duration of the

radial flow regime identified in the transient responses, where the duration is limited by the shortest response. The indicators in Table 4 are estimated at the end of the highlighted period

**Table 4** Comparison of the manual PTA interpretation (model-based, the metrics (14)) and the PTA-metrics (10) results for dimensionless well ( $PI$  and  $WPI$ ), reservoir ( $kh$  and  $RPI$ ) and connection ( $dP$  (Skin) and  $CPI$ ) performances for the analysis illustrated in Figs. 10, 11

Transients compared	Well performance		Reservoir performance		Connection performance	
	Model-based	PTA-metrics	Model-based	PTA-metrics	Model-based	PTA-metrics
Step 8	1.00	1.00	1.00	1.00	1.00	1.00
Step 9	0.99	0.97	1.05	1.03	0.95	0.94
Step 11	1.22	1.16	1.37	1.36	0.90	0.86
Step 12	1.23	1.03	1.85	1.70	0.71	0.61
Step 14	1.97	1.77	3.43	3.22	0.66	0.55

**Fig. 12** The field case used for testing the PTA-metrics from (Namazova et al. 2021). Left: top view of the reservoir with three producers (wells A-C) and injector (well D). Right: box model with simplified well and reservoir descriptions used in the analytical PTA interpretations reported in (Namazova et al. 2021)

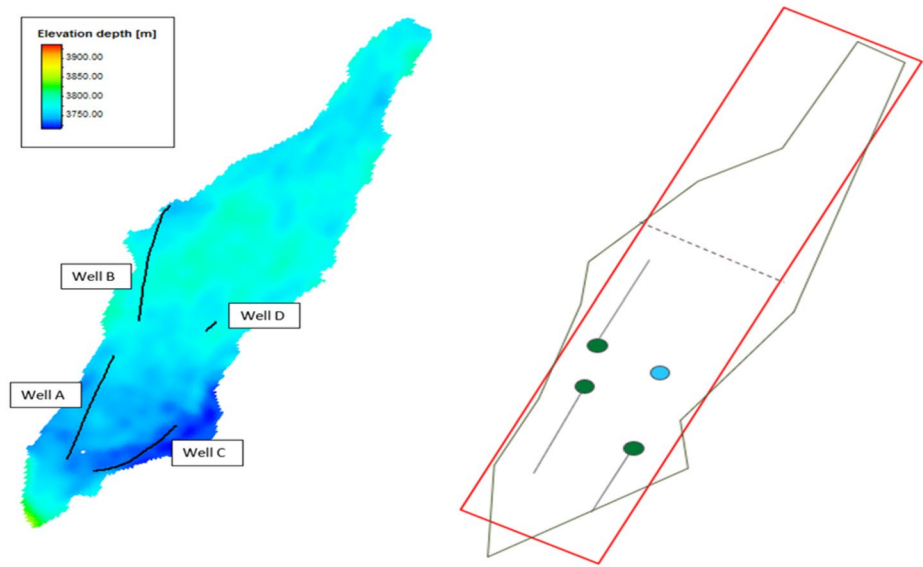


**Fig. 13** Production history of well C (Fig. 12) with time-lapse pressure build-ups (BU) measured during initial depletion (BU1 and 2) and after start of injection in well D (BU3 and 4)

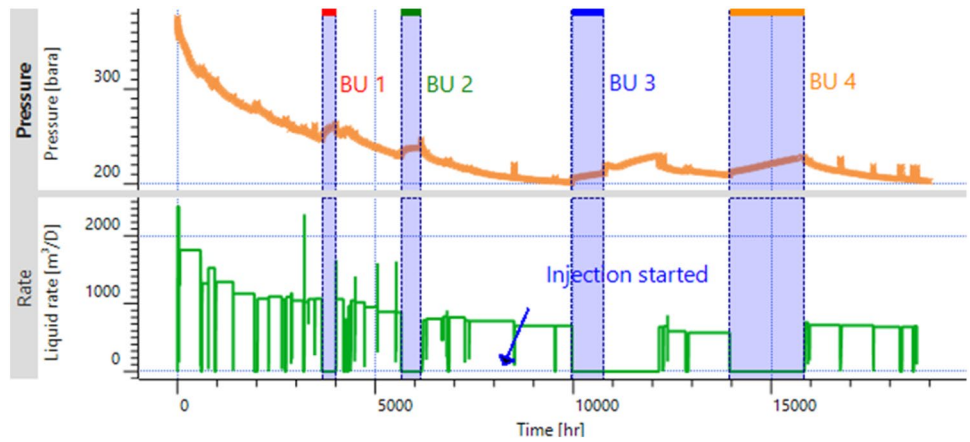


**Fig. 14** Time-lapse pressure transients and derivatives in the log–log scale for well C (BU1-4 from Fig. 13)

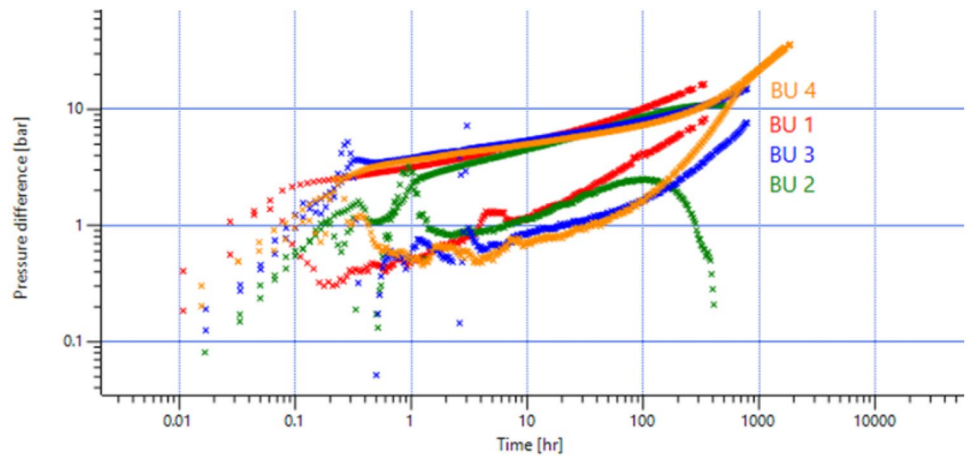
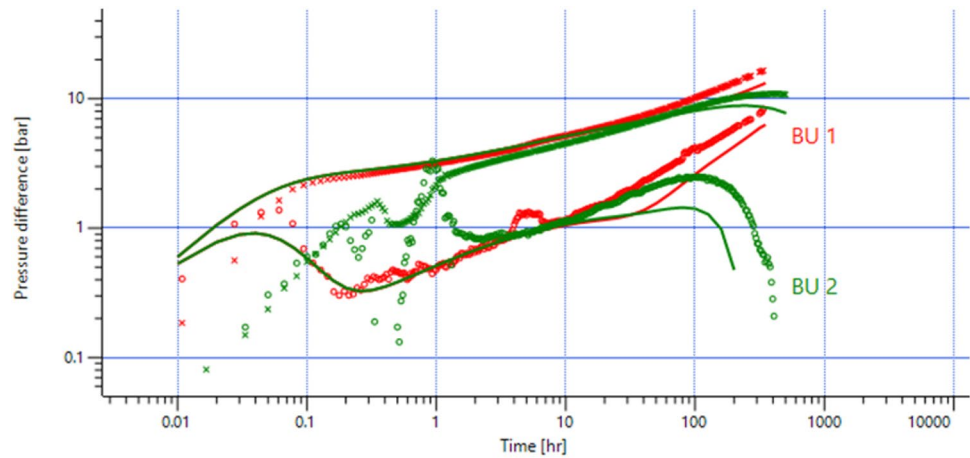


Figure 13 illustrates the production history of the well C with four time-lapse well shut-ins provided pressure build-ups (BU). These time-lapse responses, shown in

the log–log plot in Fig. 14, were selected for testing of the PTA-metrics in this paper. The analysis using conventional PTA approach and the Saphir interpretation and

**Fig. 15** Matching first and second transients (BU1 and 2) with the same kh and moderate positive skin (0.25)



**Fig. 16** Matching fourth transient (BU4) with kh and skin used for matching transients 1 and 2 (the red curves titled ‘kh (BU 1 and 2)’) and with modified kh and skin: doubled kh and increased skin of 0.7 (the orange curves titled ‘kh (BU 1 and 2) × 2’)

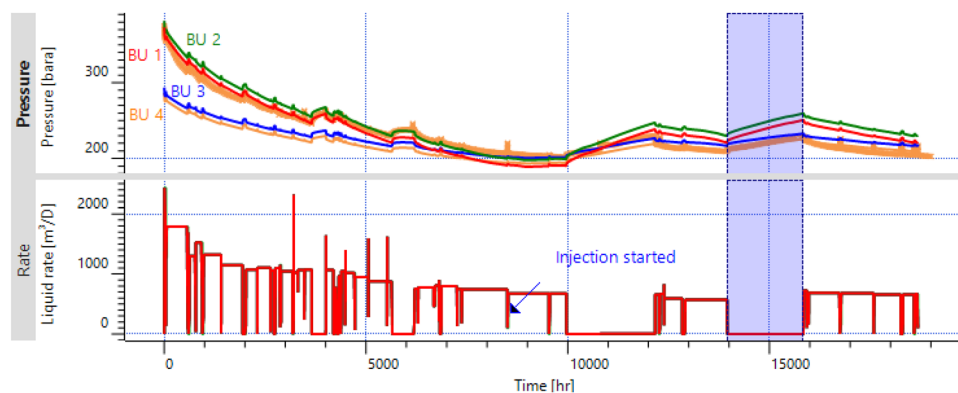
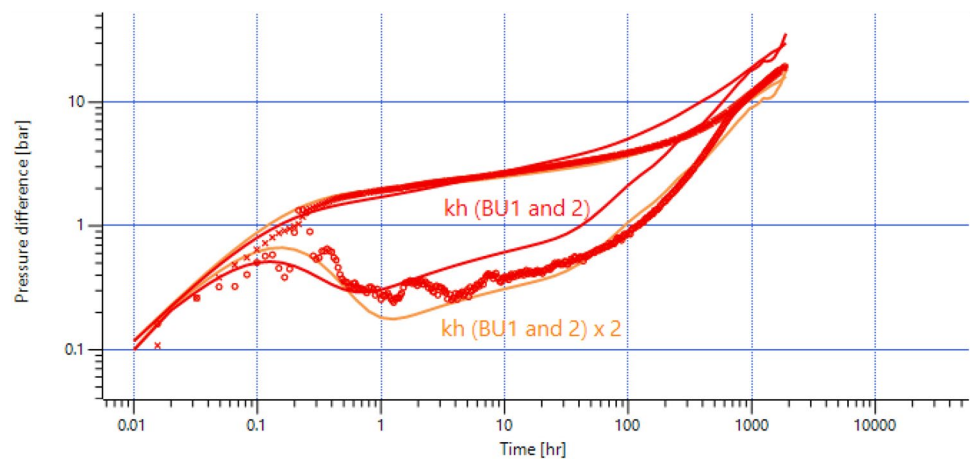


**Fig. 17** Results of matching history of well C with the box-model tuned to match first and second transients (BU1 and 2, Fig. 15) and third and fourth transients (BU3, and BU4, Fig. 16). The model tuned to BU1 and 2 fits well the depletion period, while tuned to BU3 and

4 – the period after start of the injection. The change in pressure dynamics seems to be related with connection of the bottom layer to the well drainage area (Namazova et al. 2021)

simulation tool (Molina 2020), (Namazova et al. 2021) revealed strong well interference signature in the late-time transient responses when comparing BU1 and BU2, where all producers were shut-in during BU1 and the only well C was shut-in during BU2 (Fig. 15). The analysis also suggested that injection in the well D initiated connection of the bottom layer (previously inactive) to the drainage area of well C, which was reflected in doubling of  $kh$  via doubling the pay thickness (the downward shift of the pressure derivatives comparing BU1-2 with BU3-4 responses). Doubling of  $kh$  in the analytical simulations on the box-model (Fig. 12) allowed for a reasonable match of the transient responses after start of the injection (Fig. 16). The matching of the transients also suggested some skin increase for the injection period. Figure 17 illustrates history match of the periods with depletion and water injection, where the box-model with original  $kh$  provided reasonable match of the depletion period, while doubling of  $kh$  gave a reasonable match of the injection period. It should be mentioned that the downward shift of the pressure derivatives may be also related to increase in permeability and effective well length as discussed in the last synthetic case above. This hypothesis was tested in the studies (Molina 2020), (Namazova et al. 2021) and was not prioritized due to inability to reproduce the pressure stabilization in the production history after the injection start. It should be also noted that the quality of the history matching shown in this paper is limited by the simplified box-model applied, which however captures main features of the reservoir. More complicated simulations with improved matching may be found in (Molina 2020) and (Namazova et al. 2021). The box-model with tuned parameters provided reasonable match of the transients and parts of the history, although having some deviations from the observations that should be accounted for in

further analysis. The main objective of using the history matching results was obtaining all the model parameters needed for the model-based metrics (14) and then for comparison with the PTA-metrics (10).

These four pressure transients (Fig. 14) were further evaluated using the PTA-metrics (10) in comparison with the model-based metrics (14). The PTA-metrics applied to compare the first and second transients of the well C resulted in negligible deviations of the well performance from the first to second transient (Fig. 18), if the time-window with dominating linear flow regime to the horizontal wellbore used for the comparison. This is in line with the standard interpretation results described above (Fig. 15), which have shown no tangible changes of  $kh$  and skin. However, including the late-time transient responses in calculating the performance indicators led to strong deviation of the second transient' indicators from the indicators for the first transient (Fig. 18). The late-time response here is governed by change of boundary conditions on the well drainage area in these two cases (Namazova et al. 2021). This confirmed the observation made in the previous section when discussing the results in Fig. 9: comparison of the suggested indicators is reliable for the periods of the same flow regimes in the compared transients, but may lose reliability if flow regimes are different. In our case, the late-time flow regime in the second transient is different from the regime observed for the same time in the first transient.

The PTA-metrics were then applied to compare the first, third and fourth transients. Preliminarily, a comparison of the third and fourth transients using the PTA-metrics (where third transient is considered as the reference) was carried out. The comparison did not reveal significant changes in WPI, RPI and CPI (Table 5), which is in line with the model-based interpretation. Actually, these transients are quite similar with the main flow regime (linear flow to the

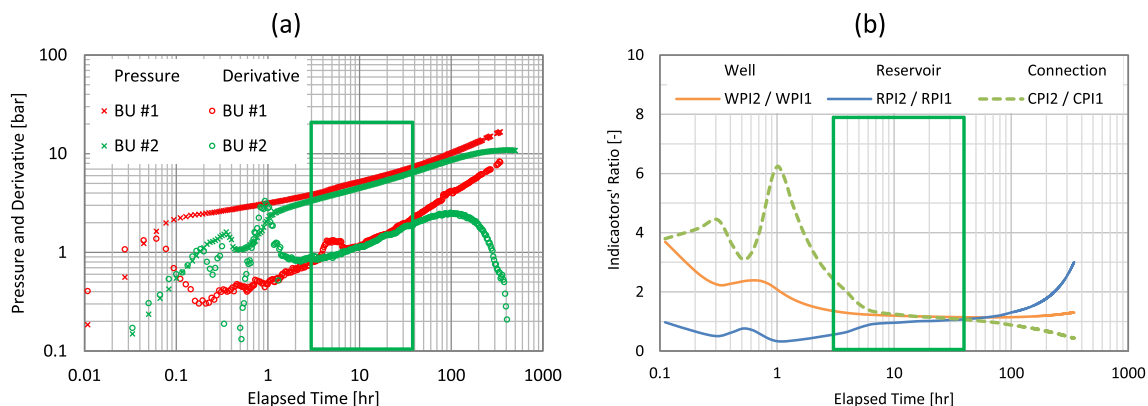


**Fig. 18** Comparison of well-reservoir performance based on the PTA-metrics for first and second transients of the well C, both during depletion period (Fig. 14): the first and second transients **a** and dimensionless well, reservoir and connection performance indicators

(WPI, RPI, CPI) for these transients (similar to Fig. 9, **b**. Dimensionless WPI, RPI and CPI at the end of the window are 1.14, 1.08 and 1.06 correspondingly

**Table 5** Comparison of model-based (14) and PTA-metrics (10) evaluations of dimensionless well, reservoir and connection performances for the results shown in Figs. 18, 19, 20 (with addition of the case of comparison of 3rd and 4th transients). Some deviations of the box-

model results from the measurements makes this comparison approximate, e.g., WPI may better reflect well performance changes than productivity index calculated from the model

Transients compared	Well performance		Reservoir performance		Connection performance	
	Model-based	PTA-metrics	Model-based	PTA-metrics	Model-based	PTA-metrics
2 and 1	0.99	1.14	$h \times 1$	1.08	1.01	1.06
3 and 1	1.14	1.01	$h \times 2$	1.59	0.72	0.64
4 and 1	1.19	1.10	$h \times 2$	1.89	0.69	0.58
4 and 3	1.05	1.09	$h \times 1$	1.18	0.95	0.92

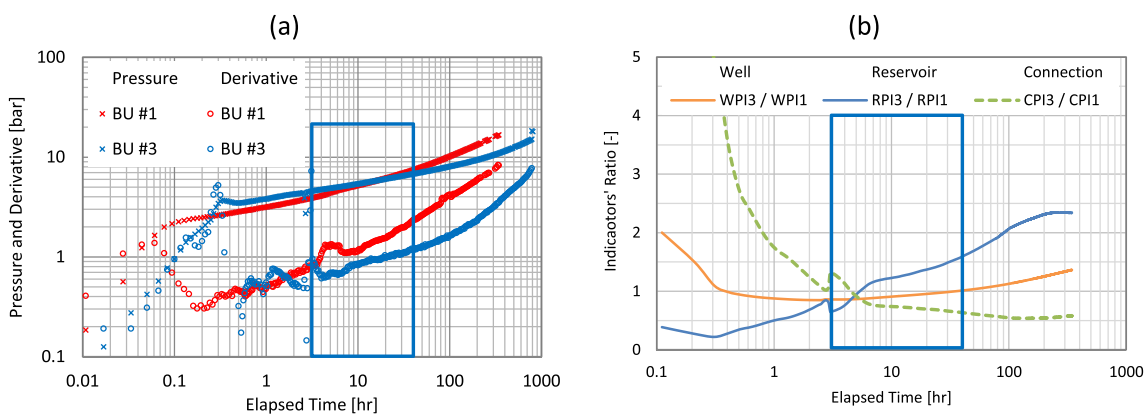


**Fig. 19** Similar well performance analysis (Fig. 18) for first and third transients of the well C, third transient is measured after injection started. Dimensionless WPI, RPI and CPI at the end of the window are 1.01, 1.59 and 0.64

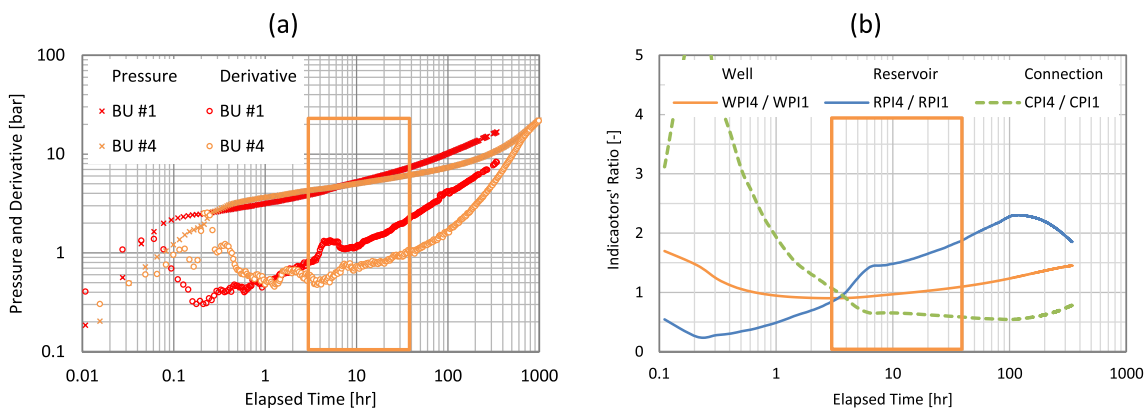


**Fig. 20** Similar well performance analysis (Fig. 18) for first and fourth transients of the well C, the fourth transient is measured after injection started. Dimensionless WPI, RPI and CPI at the end of the window are 1.10, 1.89 and 0.58

horizontal wellbore up to 40–100 h) with only difference in the late-time response (after 100 h).

The diagnostics based on time-lapse responses in the log–log plot (Fig. 14) revealed a downward shift of the pressure derivatives from first–second to third–fourth transients, while pressure drop indicated some skin increase at

the same time. In the conventional interpretation (Table 5), it resulted in doubling of  $h$  ( $kh$ ) and additional pressure drop of due to skin change. In application of the PTA-metrics, the downward shift resulted in increasing RPI and WPI and decreasing CPI proportional to those, obtained in the interpretation with conventional PTA approach

(Figs. 19, 20 Table 5). In particular, RPI changed in the range of 1.6–1.9 reflecting approximately doubling of  $h$  ( $kh$ ). It should be noted, that the RPI reaction to doubling of  $h$  in the synthetic case (Fig. 9) was accurately reflected by dimensionless RPI changed to 2.0. CPI reduction is also in line with the skin-related pressure drop change in the model-based metrics (Table 5). In general, the same RPI increase may indicate also effective well length increase as described in the synthetic case above (Fig. 9). In applications of the PTA-metrics for such cases, all potential reasons ( $k$ ,  $h$  and  $L_w$  change) should be accommodated, while one of the reasons may be chosen incorporating additional data and knowledge (as in our field case analysis).

It should be noted that all performance indicators based on the PTA-metrics vary with time (Figs. 18, 19, 20), i.e., are dependent on time-window for comparison of the transients. Therefore, choosing a proper window for such comparison, e.g., based on stabilization of derivative trends related to stabilized flow regimes (as linear flow in the case above), is crucial component of application of the PTA-metrics.

Although the ‘true solution’ is not available for the analysis of actual well measurements, a summary of comparison of the conventional PTA interpretation (model-based) with the PTA-metrics applications may be carried out based on Table 5. The comparison argues for reliability of the PTA-metrics, if a time-window with similar derivative signatures (a ‘stable pattern’) is used. In this case, the PTA-based performance evaluations are in line with the model-based interpretations. Change of flow regimes, as observed at late time (Fig. 15), reflected by the change of pressure derivative, may lead to inaccuracy of CPI and RPI evaluations with the PTA-metrics.

## Discussion

The proposed PTA-metrics are capable of revealing well performance changes and separating well and reservoir contributions using time-lapse analysis of permanent downhole and/or wellhead pressure measurements in combination with rates. The well, reservoir and connection performance indicators (WPI, RPI and CPI) are calculated using the integral-based approach providing metrics for comparison of the well performance under different conditions. Application of the metrics is quite simple and solely based on pressure and rate measurements, that makes it possible to be used in automated workflows. Noisy data or wellbore effects usually observed in real transient responses at early times should not damage the resulting performance indicators for long enough transients (in the field cases studied, duration of the early time responses with noise and WBS effect was less than 1% of the transient durations). Integrating the well measurements reduces impact of such early time

disturbances. Model independence and ability to be applied in the cases of limited well and reservoir data available may be also considered as advantages of the PTA-metrics. All the points above may argue for integrating the PTA-metrics into automated workflows and on-the-fly interpretations.

Main limitations, having impact on reliability and applicability of the metrics, are (1) stability of the pattern of time-lapse responses (e.g., derivative stabilization at radial flow or stabilization of the derivative slope at linear flow regime) and (2) sensitivity to transient duration, i.e., duration of compared transients should be similar and long enough to diminish early time pressure disturbances. The need for selecting a time-window with stable time-lapse pattern for the PTA-metrics application makes human interaction necessary in general case. As an intermediate solution, the window may be selected based on time-lapse responses in initial period and then kept the same. Thus, in the field case above, the selection of the 40 h window, done based on analysis of the first two transients, may be further used for the third and fourth transients. At the same time, the ultimate goal may be a fully automated approach where time-window is also automatically selected, e.g., based on recognition of patterns in the time-lapse pressure responses.

## Conclusions

PTA-metrics have been proposed to analyze changes in well (WPI), reservoir (RPI) and well-reservoir connection (CPI) performances from time-lapse pressure transient responses. The metrics application area includes the cases of dominating low-compressible single-phase flow in a reservoir such as initial oil production before water- or gas-breakthrough or water injection after forming of an injection pattern. Input data for the well performance monitoring using the metrics are permanent well pressure measurements in combination with flow rates.

The metrics originate from analysis of the vertical wells with dominating radial flow regime and has been verified using different synthetic cases for such wells. This was followed by a field case verification for a slanted fractured well. The verification was carried out via comparison of the PTA-metrics results with the PTA interpretation results obtained with the conventional model-based approach.

The following conclusions may be drawn for vertical/slanted wells:

- The metrics demonstrated high accuracy in all the synthetic cases as well as in the field case with the average errors less than 5% for synthetic and 10% for field cases.



- The metrics application depends on a presence of radial flow regime in all compared transients, although this is a general precondition in PTA interpretations for such wells. Radial flow may be easily identified from the derivative stabilization, making manual and automated identification quite simple.

An extension of the PTA-metrics application area was then explored with simulation and interpretation of horizontal well responses. A testing on a synthetic case was followed by a field case, where the same comparison technique described above was employed.

The confident results of the verification above for the vertical well cases were moderated in the case of the horizontal wells:

- The synthetic well cases disclosed some deviation in changes of RPI from changes of the governing parameters. Thus, doubling of reservoir parameters including permeability, pay thickness or effective well length have resulted in RPI of 1.6, 2.0 and 1.7 correspondingly (in contrast with the vertical well cases with RPI 1.9–2.0 for similar case of doubling flow capacity). WPI and CPI behaved similarly to the case of vertical wells for the cases of permeability and well length, but deviated for the case of thickness change.
- Similar results were obtained in the field case analysis, where the PTA-metrics showed reasonable agreement with the conventional PTA interpretation (with the average deviations of about 10%).
- Analysis of the field case also revealed strong sensitivity of the metrics results to the time-window, which should be selected based on recognition of stable pressure and derivative pattern.

The following three advantages and one limitation of the PTA-metrics may be highlighted based on the study:

- The performance indicators (WPI, RPI and CPI) suggested are model-independent, i.e., there is no need for choosing and assembling of a well-reservoir model as it's done in common practice, neither matching of the model to observed data.
- The above point also avoids the need for detailed input for the model including well, fluid and reservoir data. All these make the metrics proper candidates for application in automated well surveillance workflows, also providing possibility for on-the-fly interpretation enabling early alarms on performance issues.
- The tests on the field data have also shown low sensitivity of the PTA-metrics to noise in pressure data governed by the integral approach applied.

- The time-dependence of the performance indicators and window-based application procedure are the main limitations in application of the metrics. Further studies of different patterns of time-lapse pressure responses in the log–log scale may help to extend the scope and improve the reliability of the metrics applications.

The PTA-metrics presented in this paper may be used as a physics-based component of a hybrid automated well monitoring workflow in combination with a pattern recognition technique, providing proper time-windows for the metrics application. Such workflow may be further integrated in an automated decision making and predictive well maintenance with timely alarming on performance issues. As an alternative, the metrics are ready to be used in a semi-supervised manner, where the time-windows are selected with human interaction, at least for a part of analyzed data set. The metrics were successfully tested on pressure transients from both well flowing and shut-in periods encouraging analysis of all available transient data in the well monitoring workflows.

Monitoring the well performance using the metrics, including well history and on-the-fly analyses, may function as a preliminary step for the standard PTA interpretation. Here, the engineers may concentrate on selected transient data and carry out detailed analysis with the standard PTA based on the performance issues alarmed by the metrics, reducing time and resources used.

**Acknowledgements** ConocoPhillips Skandinavia and Wintershall Dea Norge are acknowledged for providing access to the field cases first analyzed in (Shchipanov et al. 2017b) and (Molina 2020), (Namazova et al. 2021) and used in this study as examples. Kappa Eng. is acknowledged for access to academic license of Kappa Workstation. The interpretations and conclusions presented in this paper are those of the authors and not necessarily those of the industry partners of the AutoWell project. The authors are grateful to the anonymous reviewers for their comments and suggestions which helped to improve the manuscript.

**Funding** The authors acknowledge the AutoWell project funded by the Research Council of Norway and the industry partners including ConocoPhillips Skandinavia, Lundin Energy Norway, Sumitomo Corporation Europe Norway Branch, Wintershall Dea Norge and Aker BP (Grant No. 326580) for support in preparation and publishing of this paper.

## Declarations

**Conflict of interest** The authors declare that they have no known competing financial interests or personal relationships that could have appeared to influence the work reported in this paper.

**Open Access** This article is licensed under a Creative Commons Attribution 4.0 International License, which permits use, sharing, adaptation, distribution and reproduction in any medium or format, as long as you give appropriate credit to the original author(s) and the source, provide a link to the Creative Commons licence, and indicate if changes were made. The images or other third party material in this article are included in the article's Creative Commons licence, unless indicated

otherwise in a credit line to the material. If material is not included in the article's Creative Commons licence and your intended use is not permitted by statutory regulation or exceeds the permitted use, you will need to obtain permission directly from the copyright holder. To view a copy of this licence, visit <http://creativecommons.org/licenses/by/4.0/>.

## References

- Aamodt G, Abbas S, Arghir D, Frazer L, Mueller D, Pettersen P, Mebratu A (2018) Identification, problem characterization, solution design and execution for a waterflood conformance problem in the Ekofisk Field—Norway (SPE-190209). In: SPE improved oil recovery conference, 14–18 April. Tulsa, Oklahoma, USA: SPE. <https://doi.org/10.2118/190209-MS>
- Blasingame T, Johnson J, Lee W (1989) Type-curve analysis using the pressure integral method (SPE-18799). In: SPE California regional meeting, April. Bakersfield, California: SPE. <https://doi.org/10.2118/18799-MS>
- Blasingame T, McCray T, Lee W (1991) Decline curve analysis for variable pressure drop/variable flowrate systems (SPE-21513). In: SPE gas technology symposium, pp 23–24 January. Houston, Texas: SPE. <https://doi.org/10.2118/21513-MS>
- Bourdet D (2002) Well test analysis: the use of advanced interpretation models. Elsevier, Amsterdam
- Cassie L, Yaich E, Singh S, Kaasa A, Jamankulov A (2018) Application of time-lapse pressure transient analysis to predict gas water contact movement and water breakthrough time: results from a reservoir off the North coast of Trinidad (SPE-191186-MS). In: SPE Trinidad and Tobago section energy resources conference, 25–26 June. Port of Spain, Trinidad and Tobago: SPE. <https://doi.org/10.2118/191186-MS>
- Champion B (2016) Wireless reservoir monitoring reducing reservoir uncertainty during barens sea appraisal—a case history for norvarg (SPE-180008). SPE Bergen one day seminar, 20 April. Bergen, Norway: SPE. <https://doi.org/10.2118/180008-MS>
- Cumming J, Wooff D, Whittle T, Gringarten A (2014) Multiwell deconvolution (SPE-166458). SPE Reserv Eval Eng 17(04):457–465. <https://doi.org/10.2118/166458-PA>
- Dominique Bourdet JA, Ayoub YM, Plard, (1989) Use of pressure derivative in well-test interpretation. SPE Form Eval 4(02):293–302. <https://doi.org/10.2118/12777-PA>
- Gringarten A (2008) From straight lines to deconvolution: the evolution of the state of the art in well test analysis (SPE-102079). SPE Reserv Eval Eng. <https://doi.org/10.2118/102079-PA>
- Gringarten A, von Schroeter T, Rolfsvaag T, Bruner J (2003) Use of downhole permanent pressure gauge data to diagnose production problems in a north sea horizontal well (SPE-84470). In: SPE Annual technical conference and exhibition, pp 5–8 October. Denver, Colorado: SPE. <https://doi.org/10.2118/84470-MS>
- Guo Y, Mohamed I, Zidane A, Panchal Y, Abou-Sayed O, Abou-Sayed A (2021) Automated pressure transient analysis: a cloud-based approach. J Petrol Sci Eng 196:1–16. <https://doi.org/10.1016/j.petrol.2020.107627>
- Horne RN (2007) Listening to the reservoir—interpreting data from permanent downhole gauges. J Petrol Technol 59(12):78–86. <https://doi.org/10.2118/103513-JPT>
- Houze O, Viturat D, Fjaere O (2020) Dynamic data analysis. KAPPA Larsen L (2005) Uncertainties in standard analyses of boundary effects in buildup data (SPE-90236). SPE Reserv Eval Eng 08(05):437–444. <https://doi.org/10.2118/90236-PA>
- Mimoun JG, Fernández-Ibáñez F (2023) Carbonate excess permeability in pressure transient analysis: a catalog of diagnostic signatures from the Brazil Pre-Salt. J Petrol Sci Eng 220:111173. <https://doi.org/10.1016/j.petrol.2022.111173>
- Molina J (2020) Multi-well interference test analysis, master thesis. Stavanger: UiS
- Moosavi S, Qajar J, Riazi M (2018) A comparison of methods for denoising of well test pressure data. J Petrol Explor Prod Technol. <https://doi.org/10.1007/s13202-017-0427-y>
- Namazova G, Molina J, Shchipanov A (2021) Evaluation of well interference and injection performance from analysis of time-lapse pressure transients. In: 82nd EAGE annual conference and exhibition, pp 18–21 October. Amsterdam: EAGE. <https://doi.org/10.3997/2214-4609.202113102>
- Rushatmanto M, Sianturi J, Suwito E, Priskila L (2017) Integration of time-lapse pressure transient analysis in reservoir characterization and reducing uncertainty of initial gas-in-place estimation: a case study in gas condensate reservoir (SPE-186873-MS). In: SPE/IATMI Asia Pacific Oil and gas conference and exhibition, pp 17–19 October. Jakarta, Indonesia: SPE. <https://doi.org/10.2118/186873-MS>
- Shchipanov A, Berenblyum R, Kollbotn L (2014) Pressure transient analysis as an element of permanent reservoir monitoring (SPE-170740). In: SPE annual technical conference and exhibition, pp 27–29 October. Amsterdam, The Netherlands. <https://doi.org/10.2118/170740-MS>
- Shchipanov A, Kollbotn L, Berenblyum R (2017a) Integrating pressure transient analysis into history matching. In: 79th EAGE conference and exhibition 2017a, pp 12–17 June. Paris: EAGE. <https://doi.org/10.3997/2214-4609.201700995>
- Shchipanov A, Kollbotn L, Prosvirnov M (2017b) Step rate test as a way to understand well performance in fractured carbonates (SPE-185795). In: SPE Europec featured at 79th EAGE annual conference and exhibition, pp 12–17 June. Paris, France. <https://doi.org/10.2118/185795-MS>
- Skrettingland K, Giske N, Johnsen J.-H, Stavland A (2012) Snorre in-depth water diversion using sodium silicate - single well injection pilot (SPE-154004). In: SPE improved oil recovery symposium, pp 14–18 April. Tulsa, Oklahoma. <https://doi.org/10.2118/154004-MS>
- Skrettingland K, Dale E, Roine Stenerud V, Lambertsen A, Nordaas Kulkarni K, Fevang O, Stavland A (2014) Snorre in-depth water diversion using sodium silicate - large scale interwell field pilot (SPE-169727). In: SPE EOR conference at oil and gas West Asia, 31 March–2 April. Muscat, Oman: SPE. <https://doi.org/10.2118/169727-MS>
- Suleen F, Oppert S, Chambers G, Libby L, Carley S, Alonso D, Olayomi J (2017) Application of pressure transient analysis and 4D seismic for integrated waterflood surveillance- a deepwater case study. In: SPE Western Regional Meeting, pp 23–27 April. Bakersfield, California: SPE. <https://doi.org/10.2118/185646-MS>
- Suzuki S (2018) Using similarity-based pattern detection to automate pressure transient analysis (SPE-193285). In: Abu Dhabi international petroleum conference and exhibition, pp 12–15 November. Abu Dhabi, UAE: SPE. <https://doi.org/10.2118/193285-MS>
- Ugoala O, Gad K, Whittle T, Stone M, Butter M, Galal S, Mahmoud H (2013) Time lapse PTA to determine the impact of skin, reservoir compaction, and water movement on well productivity loss: a field example from WDDM, Egypt (SPE-164668). In: SPE North Africa technical conference and exhibition, pp 15–17 April. Cairo, Egypt: SPE. <https://doi.org/10.2118/164668-MS>
- Walker H, Shchipanov A, Selseng H (2021) Interpretation of permanent well monitoring data to improve characterization of a giant oil field. In: SPE Europec featured at 82nd EAGE conference and exhibition, pp 18–21 October. Amsterdam, The Netherlands: SPE. <https://doi.org/10.2118/205148-MS>
- Whittle T, Jiang H, Young S, Gringarten A (2009) Well production forecasting by extrapolation of the deconvolution of well test

- pressure transients (SPE-122299). In: EUROPEC/EAGE conference and exhibition, pp 8–11 June. Amsterdam, The Netherlands: SPE. <https://doi.org/10.2118/122299-MS>
- Yaich E, Robertson N, Whittle T, Jamankulov A (2012) Use of pressure transient analysis for the detection of gas/water contact movement in a gas reservoir (SPE-158827). In: SPETT 2012 energy conference and exhibition, 11–13 June. Port-of-Spain, Trinidad: SPE. <https://doi.org/10.2118/158827-MS>
- Zhang B, Muradov K, Dada A (2021) Principal component analysis-assisted selection of optimal denoising method for oil well transient data. *J Petrol Explor Prod Technol* 11:509–530. <https://doi.org/10.1007/s13202-020-01010-3>

**Publisher's Note** Springer Nature remains neutral with regard to jurisdictional claims in published maps and institutional affiliations.